

Direct synthesis, characterization and catalytic application of SBA-15 containing heteropolyacid $H_3PW_{12}O_{40}$

Lina Yang^a, Yutai Qi^{a,*}, Xingdong Yuan^b, Jian Shen^b, Jiman Kim^c

^a Department of Applied Chemistry, Harbin Institute of Technology, Harbin 150001, China

^b Department of Petrochemical Technology, Liaoning University of Petroleum and Chemical Technology, Fushun 113001, China

^c Functional Materials Laboratory, Department of Molecular Science and Technology, Ajou University, Suwon 442 749, Republic of Korea

Received 28 June 2004; received in revised form 21 November 2004; accepted 23 November 2004

Available online 12 January 2005

Abstract

Phosphotungstic acid (HPWA) has been introduced into the mesoporous molecule sieve SBA-15 by a sol–gel technique. The samples were characterized by XRD, BET, FT-IR, XRF and NH_3 -TPD. The effects of the polar solvent on the hydrothermal stability have been comprehensively studied by washing the samples with an EtOH/ H_2O mixture and conducting esterification involving polar solvents. Although the acid amount of the fresh impregnated catalyst was superior to the sol–gel counterpart, the sol–gel derived composite is more stable in the acidic property and the structural regularity of the mesoporous material than the impregnated sample. Catalysis tests including reusability of the samples also prove that the sol–gel derived composite is more suitable for the use for heterogeneous catalysis.

© 2004 Elsevier B.V. All rights reserved.

Keywords: Sol–gel method; SBA-15; Phosphotungstic acid; Catalysis stability

1. Introduction

Heteropolyacids (HPA) have been extensively used as acid and oxidation catalysts for many reactions and gained application in industrial practice of both electrophilic catalysis and oxidation reactions [1–4]. HPA are insoluble in non-polar solvents and therefore, can be considered as environmentally friendly materials, being promising solid acids to replace environmentally harmful liquid acid catalysts such as H_2SO_4 and HF [5]. A main disadvantage, however, is their very low surface area ($<10\text{ m}^2\text{ g}^{-1}$), which limits their application; as a result it is necessary to disperse the HPA onto the supports having large surface area. Acidic or neutral substances such as SiO_2 , active carbon, acidic ion-exchange resin, etc. are all

suitable supports, but SiO_2 , which is relatively inert towards HPA, is the most often used [8].

Recently, mesoporous molecular sieve MCM-41 containing HPWA has been synthesized by post-synthesis and identified as a promising solid acid catalyst for conversion and formation of large organic molecules [6–8]. SBA-15 is a newly discovered mesoporous silica molecular sieve with uniform tubular channels whose pore diameter is variable from 50 to 300 Å. Compared with MCM-41, SBA-15 has larger pore diameter, thicker pore wall and higher hydrothermal stability [9]. There are few papers about the modification and application of SBA-15 with heteropolyacid [10,11].

In this paper, we focus on (1) direct synthesis of SBA-15 containing phosphotungstic acid by a sol–gel technique, (2) comparison of the structure between sol–gel derived sample and impregnated sample, and (3) comparison of the stability of the mesoporous structure and acidic properties between two samples.

* Corresponding author. Tel.: +86 4136860830; fax: +86 4136860967.

E-mail address: lnqdsd@yahoo.com.cn (Y. Qi).

2. Experimental

2.1. Synthesis of sol–gel derived 12-phosphotungstic acid SBA-15

Tetraethoxysilane (TEOS, 8.48 g) was dissolved in a mixture of 4.0 g P123 (triblock poly(ethylene oxide)–poly(propylene oxide)–poly(ethylene oxide) (EO₂₀PO₇₀EO₂₀)) and 25.1 g HCl (36 wt.%) while stirring at 313 K in an water bath. To this solution HPWA was added in a calculated amount to reach 0.88 mol% heteropolyacid loading in the final sample.

The gel composition was SiO₂:HPWA:P123:HCl:H₂O = 4.07:0.036:0.7:2.4:544. This gel was stirred for 24 h at 313 K, and then aged in a propylene vessel at 373 K for 24 h. Then the white precipitate solid was dried in vacuum oven at 383 K overnight. The dried precipitate was calcined in air for 5 h at 723 K to decompose the template and give a white powder. The final sample is labeled SG.

2.2. Synthesis of supported 12-phosphotungstic acid SBA-15

The synthesis process of all silica SBA-15 was described elsewhere [12]. The calcined all silica SBA-15 was dissolved in 150 ml water solution of calculated amount of heteropolyacid to reach 0.88 mol% heteropolyacid loading in the final sample. After stirring for 4 h at ambient temperature, the sample was dried overnight at 383 K and calcined at 723 K for 5 h. The sample is labeled IM.

2.3. Preparation of the mixture of SBA-15 and HPWA sample

SBA-15 and calculated amount of HPWA were ground to produce a 0.88 mol% heteropolyacid physical mixture. The sample is labeled PM.

2.4. Characterization

Elemental analysis of samples was performed by means of X-ray fluorescence analysis (XRF). XRD patterns were recorded between $2\theta = 0.7\text{--}5.0^\circ$ and $2\theta = 5.0\text{--}40.0^\circ$, respectively, on a Rigaku D/max-RB diffractometer instrument operating at 40 kV and 100 mA with Cu target K α -ray irradiation. N₂ adsorption–desorption were measured at 77 K on a micromeritics ASAP 2400 volumetric system, with the samples outgassed for 16 h at 383 K in vacuum (10^{-6} Torr) prior to measurement.

FT-IR spectra were measured using a Nicolet 5Dx-FT-IR spectrometer at room temperature. Analyses were performed using KBr pellet technique with a resolution at 4 cm^{-1} . Prior to measurements the samples were pretreated at 573 K for 2 h in vacuum (better than 10^{-5} Torr) or in flowing helium.

NH₃-TPD measurements were carried out with 200 mg samples on a multitask TPD system (TP-5000, China). After pretreatment in He (773 K , 30 ml min^{-1} , 1 h), the samples were exposed to ammonia at 298 K for 0.5 h then purged with helium for 1 h. TPD spectra were registered between 298 and 873 K (temperature ramp: 10 K min^{-1}) and the desorbed gases were analyzed using the integrated gas chromatography with a TCD detector. The total acid amount of the samples was calculated based on the amount of used NaOH (0.01 mol L^{-1}) titrating the solution of HCl (0.01 mol L^{-1}) containing the desorbed ammonia.

2.5. Hydrothermal treatment

Certain amount of samples were washed in the Soxhlet extractor with 95 wt.% ethanol water mixture under reflux temperature for some time, and then the samples were filtered and dried for characterization and further treatment.

2.6. Catalysis testing

The catalytic activities of samples were tested in the esterification involving acetic acid and alcohol performed in a flask with a condenser at the reflux temperature. The mol ratio of alcohol to acid was 2:1, the catalyst was 1.5 wt.% of the feed, and the reaction time was 6 h. After the reaction, the catalysts were filtered, dried, and reused. Analyses of the reaction products were performed via a HP4890D gas chromatograph.

3. Results and discussion

3.1. Characterization

3.1.1. XRD

The XRD patterns of pure SBA-15, SG, IM and PM are shown in Fig. 1. For all the samples the hexagonal structure of SBA-15 is confirmed by a typical XRD pattern consisting of a strong peak (at 2θ around 0.8°) along with two weak peaks (at 2θ around 1.6° and 1.8°) [13]. For the XRD pattern of the SG sample, diffraction from (1 0 0) plane is shifted to lower 2θ angles, indicating an increase in d-spacing, possibly due to swelling of the surfactant micelles arising from the strong interaction between the HPWA and surfactant during the hydrothermal process. In contrast, the XRD pattern of IM reveals a shift of the diffraction peaks to larger 2θ angles, i.e. a decrease in d-spacing. This is probably due to restructuring of silica during the step of adsorption of HPWA in water solution. The XRD pattern of PM, a physical mixture, is the same as that of pure SBA-15 except for the decrease in the intensities of the peaks due to the existence of HPWA.

The intensities of d_{100} , d_{110} and d_{200} of SG and IM are lower than those of pure SBA-15 because of the existence of HPWA. The diffractions from (1 1 0) to (2 0 0) planes for both materials appear as broad weak peaks, indicating the loss of

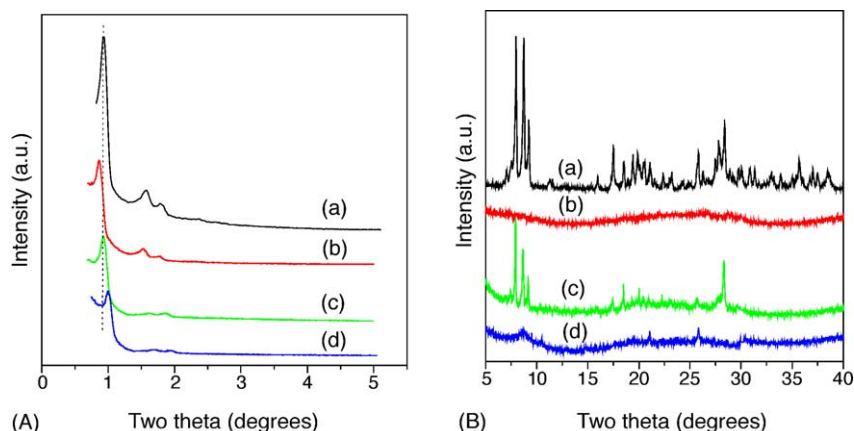


Fig. 1. Powder X-ray diffraction patterns of (A) SBA-15(a), SG (b), PM(c), IM(d) and (B) HPWA(a), SG(b), PM(c), IM(d).

long-range order. Generally, SG has higher long-range order than IM.

According to the large angle XRD patterns ($2\theta = 5\text{--}40^\circ$), no characteristic peaks of HPWA are observed for the SG sample, indicating that HPWA is probably finely dispersed on the surface of the sample or incorporated in the pore wall of the sample. However, more appreciable characteristic peaks are observed for the IM sample, indicating small quantity of crystallites of HPWA existing on the surface of IM [14]. The PM sample made by mixing the SBA-15 with HPWA has the complete structure of HPWA.

Here it can be concluded that there are chemical interactions between the host SBA-15 and the guest HPWA molecules for both SG and IM samples, and that the interactions are different from each other.

3.1.2. BET

The N_2 adsorption–desorption isotherms for pure SBA-15, SG, and IM are exhibited in Fig. 2. All the N_2 adsorption–desorption isotherms are the type of IV in nature according to the IUPAC classification and exhibited an H1 hysteresis loop which is a characteristic of mesoporous solids [15]. The adsorption branch of each isotherm showed a sharp inflection at $P/P^\circ = 0.60\text{--}0.80$, which means a typical capillary condensation within uniform pores. The position of the inflection point is clearly related to the diameter of the mesopore, and the sharpness of this step indicates the uniformity of the mesopore size distribution. The inset in Fig. 2 shows that all the samples have narrow pore size distribution within the mesopore range.

The textual properties of the IM and SG samples are listed in Table 1, it is shown that the introduction of HPWA decreases the BJH surface area, total pore volume and pore size of pure SBA-15. Such decrease is sharp for the IM sample, due to large quantity of HPWA existing in the channel, on the surface or on the pore wall. However, the decrease for the SG sample is much smaller than the IM sample, probably due to the existence of considerable amount of HPWA in the pore wall of the SG sample.

3.1.3. FT-IR

Fig. 3 shows the FT-IR spectra of the samples in the region $1200\text{--}600\text{ cm}^{-1}$ [11]. Bands observed at 1083 , 982 , 890 and 808 cm^{-1} , which are the fingerprint of the Keggin structure of HPWA, are usually assigned to $\nu_{as}(\text{P}\text{--}\text{O})$, $\nu_{as}(\text{W}\text{=}\text{O})$, $\nu_{as}(\text{W}\text{--}\text{O}_b\text{--}\text{W})$ in corner shared octahedral, and $\nu_{as}(\text{W}\text{--}\text{O}_c\text{--}\text{W})$ in edge shared octahedral [16], respectively. These characteristic bands are regarded as experimental evidences for the existence of HPWA molecules or molecular fractions such as phosphorous oxides and/or tungstate ions. According to the spectra of the SG and IM samples, they can both retain the characteristic peaks of HPWA. However, their spectra are significantly different from each other, stronger characteristic peaks (W=O and W–O_c–W) of the SG sample indicate that the Keggin structure is more retained than IM sample. Compared with the spectra of bulk HPWA, red shifts of ν_{as}

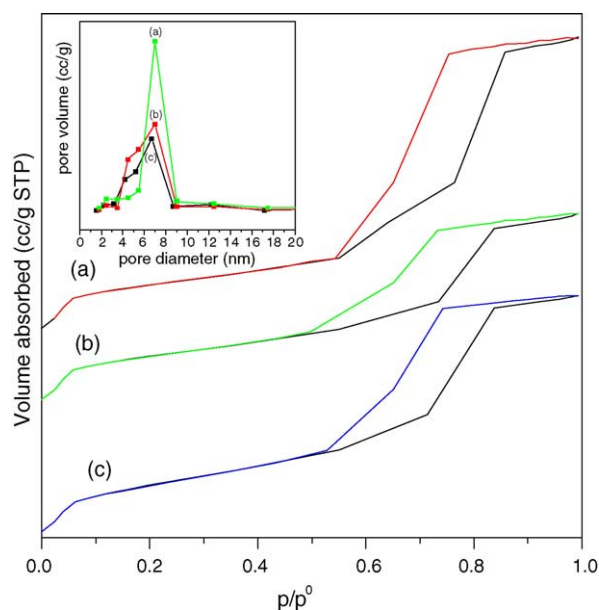


Fig. 2. The N_2 adsorption isotherm of SBA-15(a), SG(b) and IM(c).

Table 1
Textual property of the samples

Sample	d_{100} (Å)	a_0^a (Å)	S_{BJH} ($\text{m}^2 \text{g}^{-1}$)	V_{BJH} (cm^3/g)	D_{BJH} (Å)
SBA-15	101.03	116.68	801.00	0.93	72.00
SG	102.71	118.60	577.98	0.85	59.44
IM	88.33	101.99	469.72	0.68	56.66
SGW ^b	99.65	115.07	631.98	0.92	58.23
IMW ^c	85.67	98.92	658.29	0.93	56.51
SGR ^d	–	–	623.82	0.91	58.35
IMR ^e	–	–	636.60	0.90	56.55

^a a_0 was determined from the d_{100} , where $a_0 = 2/(3)^{1/2}d_{100}$.

^b SG after EtOH/H₂O treatment for 24 h.

^c IM after EtOH/H₂O treatment for 24 h.

^d SG after esterification for 4 times.

^e IM after esterification for 4 times.

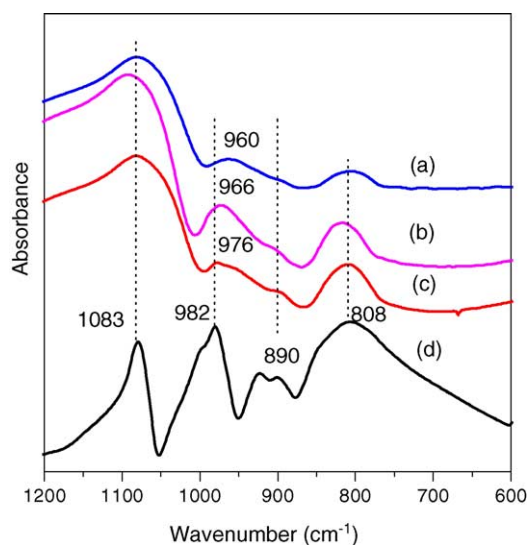


Fig. 3. FT-IR spectra of SBA-15(a), SG(b), IM(c) and HPWA(d).

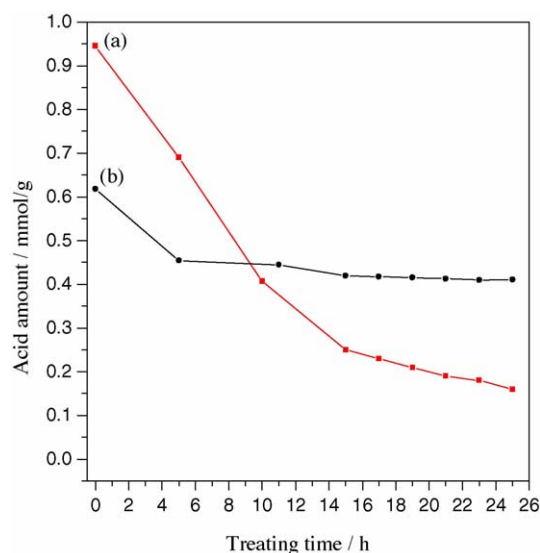


Fig. 5. Acidity changes of two samples washed with EtOH/H₂O mixture of IM(a) and SG(b).

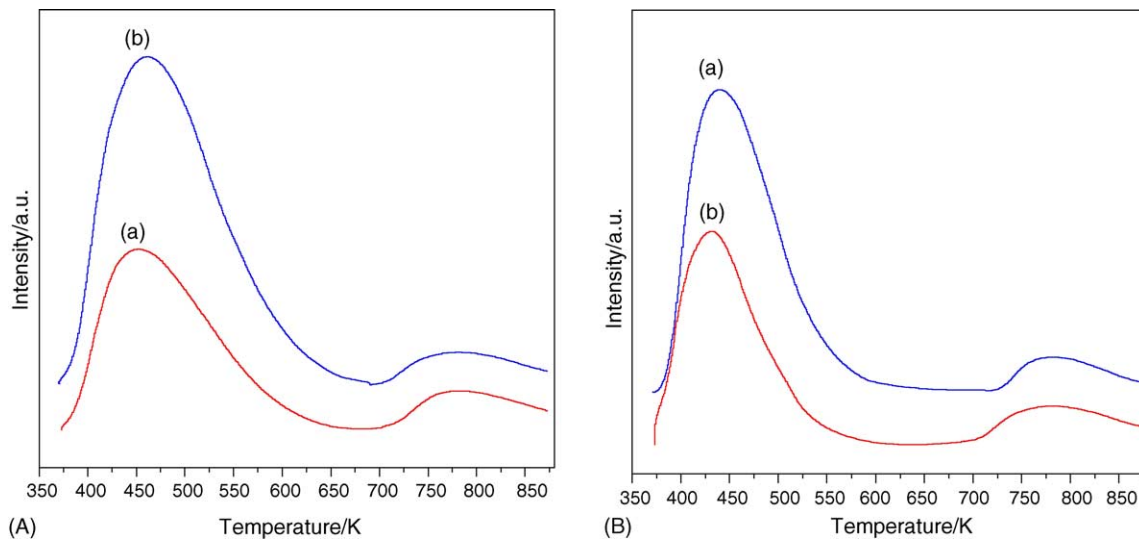


Fig. 4. NH₃-TPD of (A) SG(a), IM(b) and (B) SGW(a), IMW(b).

Table 2
Acidic properties of the samples

Sample	HPWA (mol%) (calculated)	HPWA (mol%) (found)	Acid sites amount (mmol/g)	T_{\max} (°C)
SBA-15	0.00	0.00	0.0204	–
SG	0.88	0.64	0.62	~505
IM	0.88	0.85	0.95	~505
SGW	–	0.43	0.41	~503
IMW	–	0.12	0.16	~504
SGR	–	0.40	0.43	~503
IMR	–	0.11	0.17	~505

The amount of desorpted NH_3 represents the acid sites amount. T_{\max} (°C) represent the acid strength of the catalysts.

(W=O) for the SG and IM samples prove the intense chemical interaction between HPWA and SBA-15. The shift of SG is more remarkable than IM, and thus it can be concluded that stronger interaction exists between HPWA and SBA-15 for the SG sample.

3.1.4. NH_3 -TPD and XRF

The acid properties including acidic sites amount and acid strength of catalysts were studied with NH_3 -TPD, and the spectra of the samples are shown in Fig. 4. Fig. 4A shows that both IM and SG have two characteristic peaks. An intense peak with a maximum between 454 and 459 K corresponds to desorption of weakly held, physisorbed ammonia. A wide,

much less intense peak appearing at even higher temperature represents desorption of chemisorbed ammonia. For the fresh samples, IM has a larger acid amount than SG but the acid strength of samples is similar.

XRF results are listed in Table 2. The amount of HPWA found in SG is less than that in IM possibly due to the reaction between surfactant and HPWA during the synthesis of the SG sample.

3.2. Hydrothermal stability testing

The hydrothermal stabilities of the samples were tested by characterizing the changes of the samples after hydrothermal

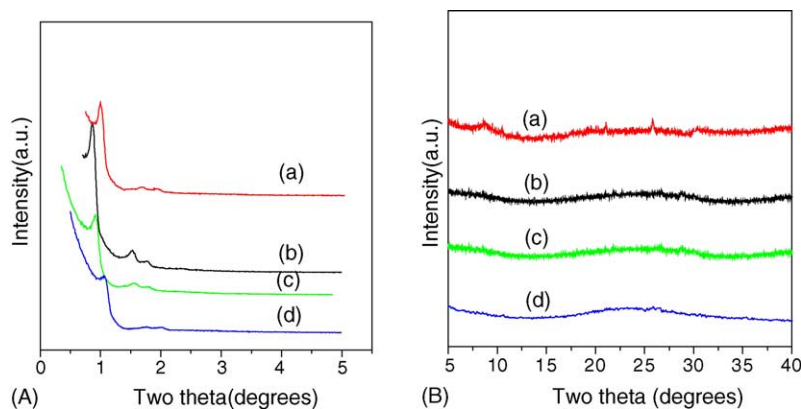


Fig. 6. Powder X-ray diffraction patterns of IM(a), SG(b), SGW(c) and IMW(d).

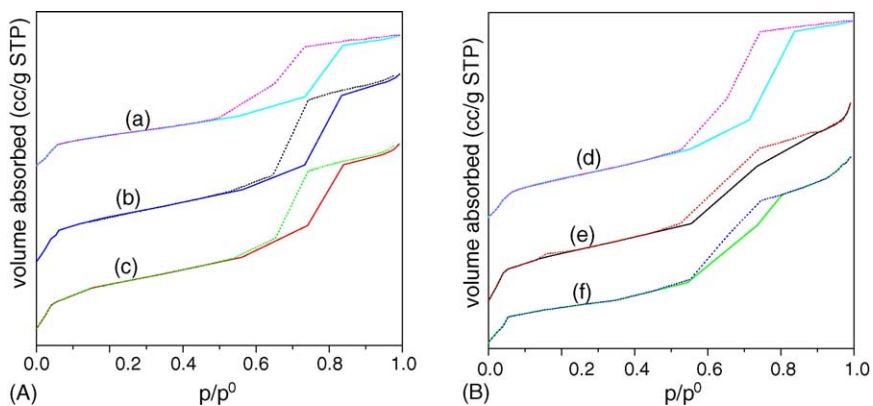


Fig. 7. N_2 adsorption isotherm of (A) SG(a), SGW(b), SGR(c) and (B) IM(d), IMW(e), IMR(f).

treatment and reaction by means of NH_3 -TPD, XRF, XRD, and BET.

3.2.1. NH_3 -TPD and XRF

The NH_3 -TPD profiles (Fig. 4B) indicate that the ratio of strong acid to weak acid increases for both samples and that IM loses acid amount more rapidly than SG under hydrothermal treatment. The detailed data are listed in Table 2.

Fig. 5 shows the changes of acid amounts of IM and SG after hydrothermal treatment. The acid sites amount of both SG and IM decreases sharply at the early time due to the easy dissolution of HPWA from the surface in the polar medium. It should be noticed that the further treatment makes the IM sample continuously lose acidity, however, the acid amount of SG can be constant after 5 h hydrothermal treatment. Apart from the surface Si–OH, the proton of HPWA can also interact with the Si–OH formed by hydrolysis of TEOS during the synthesis of the SG sample. Therefore considerable amount of HPWA is incorporated into the pore wall, and such HPWA is difficult to lose in polar solvent.

The influences of hydrothermal treatment and reaction on the composition of the samples were studied (Table 2). Changes of composition of the catalysts after hydrothermal treatment and reaction correlate well with the changes of acid sites amount.

3.2.2. XRD

The structure of the IM and SG samples washed with the EtOH/ H_2O mixture for 24 h are shown in Fig. 6. The washed SG sample (SGW) has better long-range order structure than the washed IM sample (IMW) (Fig. 6A). IMW loses the characteristic peaks completely, since HPWA dissolves easily in polar solvent, and no remarkable changes are observed for SGW (Fig. 6B, $2\theta = 5\text{--}40^\circ$).

3.2.3. BET

The influences of hydrothermal treatment and reaction on the mesoporous structure of the samples were also characterized by N_2 adsorption–desorption. No remarkable changes are observed for the isotherms of the SG sample (Fig. 7A) after hydrothermal treatment and reaction; however, the treatment and reaction make the isotherms of the IM sample (Fig. 7B) change a lot. It can be concluded here the sol–gel method is helpful for the structure stability in the system involving polar solvent. Table 1 shows that the surface area and pore volume of SG and IM increase after hydrothermal treatment and reaction due to the leaching of HPWA.

3.3. Catalytic test

Esterification between alcohol and acetic acid was used as a testing reaction (Fig. 8). Compared with almost inert SBA-15 for the reaction, both fresh IM and fresh SG can catalyze the reaction very well, and the catalytic activity of the fresh IM catalyst surpasses that of the fresh SG catalyst, because each acid site is probably accessible to the reactant.

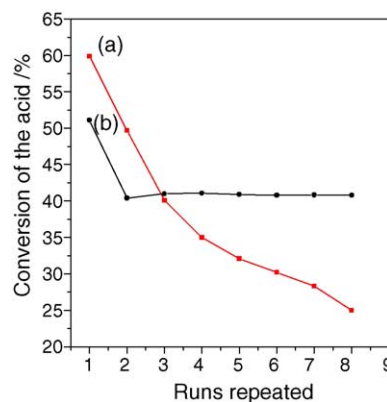


Fig. 8. Stability of IM(a) and SG(b).

The stabilities of the samples were also investigated by means of reusing the samples in the testing reaction. The IM sample loses its activity rapidly and continuously due to the easy leaching of HPWA in the reaction system. However, the activity of SG sample, after a sharp decrease at early times, is comparatively constant in further reaction. It follows from this that the IM catalyst is less stable than SG in the reaction system involving polar solvent.

4. Conclusions

Mesoporous molecule sieve SBA-15 containing HPWA has been directly synthesized by a sol–gel method. IM has higher acid amount than SG, however, SG has better stability in the system involving polar solvent than IM sample because of considerable amount of HPWA existing in the pore wall. Therefore, it can be unambiguously proved that the SG sample is a more suitable heterogeneous catalyst for the reaction involving the polar solvent.

Acknowledgements

The financial support of Liaoning University of Petroleum Chemistry and Technology is gratefully acknowledged. We are also thankful to Fushun Institute of Petrochemistry for characterizing the catalysts.

References

- [1] Y. Izumi, K. Urabe, M. Onaka, Zeolite, Clay and Heteropolyacids in Organic Reactions, Kodansha/VCH, Tokyo/Weinheim, 1992.
- [2] R.J.J. Jansen, H.M. van Veldhuizen, M.A. Schwegler, H. van Bekkum, Recl. Trav. Chim. Pay-Bas 113 (1994) 115.
- [3] T. Okuhara, N. Mizuno, M. Misono, Adv. Catal. 41 (1996) 113.
- [4] I.V. Kozhevnikov, Chem. Rev. 98 (1998) 171.
- [5] A. Molnar, C. Keresszegi, B. Torok, Appl. Catal. A: Gen. 189 (1999) 217.
- [6] W. Chu, X. Yang, X. Ye, Y. Wu, Appl. Catal. A 145 (1996) 125.
- [7] W. Chu, X. Yang, Y. Shan, X. Ye, Y. Wu, Catal. Lett. 42 (1996) 2001.

- [8] A. Molnar, T. Beregszaszi, A. Fudala, B. Torok, M. Rozsa-Tarjani, I. Kiricsi, in: B.K. Hodnett, A.P. Kybett, J.H. Clark, K. Smith (Eds.), *Supported Reagents and Catalysts in Chemistry*, The Royal Society of Chemistry, Cambridge, 1998, p. 25.
- [9] X. Yuan, J. Shen, G. Li, *Chin. J. Catal.* 23 (2002) 9.
- [10] A. Lapkin, B. Bozkaya, T. Mays, L. Borello, *Catal. Today* 81 (2003) 616–618.
- [11] A. Kukovecz, Zs. Balogi, Z. Konya, M. Toba, P. Lentz, S.-I. Niwa, F. Mizukami, A. Molnar, J.B. Nagy, I. Kiricsi, *Appl. Catal. A: Gen.* 228 (2002) 83–94.
- [12] D. Zhao, Q. Huo, J. Feng, B.F. Chmelka, G.D. Stucky, *J. Am. Chem. Soc.* 120 (1998) 6024.
- [13] Z. Luan, M. Hartmann, D. Zhao, W. Zhou, *Chem. Mater.* 11 (1999) 1621–1627.
- [14] X. Zhang, Y. Yue, Z. Gao, *Chem. J. Chin. Univ.* 22 (2001) 1169–1172.
- [15] M. Kruk, M. Jaroniec, C.H. Ko, R. Ryoo, *Chem. Mater.* 12 (2000) 1961–1968.
- [16] C. Rocchiccioli-Deltcheff, M. Fournier, R. Frank, *Inorg. Chem.* 22 (1983) 207.